



LAWRENCE
LIVERMORE
NATIONAL
LABORATORY

UCRL-CONF-234101

Effect of Organic Acid Additions on the General and Localized Corrosion Susceptibility of Alloy 22 in Chloride Solutions

Ricardo M. Carranza, C. Mabel Giordano, Martín A. Rodríguez, Gabriel O. Ilevbare, Raul B. Rebak

August 29, 2007

Scientific Basis for Nuclear Waste Management XXXI
Sheffield, United Kingdom
September 16, 2007 through September 21, 2007

Disclaimer

This document was prepared as an account of work sponsored by an agency of the United States Government. Neither the United States Government nor the University of California nor any of their employees, makes any warranty, express or implied, or assumes any legal liability or responsibility for the accuracy, completeness, or usefulness of any information, apparatus, product, or process disclosed, or represents that its use would not infringe privately owned rights. Reference herein to any specific commercial product, process, or service by trade name, trademark, manufacturer, or otherwise, does not necessarily constitute or imply its endorsement, recommendation, or favoring by the United States Government or the University of California. The views and opinions of authors expressed herein do not necessarily state or reflect those of the United States Government or the University of California, and shall not be used for advertising or product endorsement purposes.

Effect of Organic Acid Additions on the General and Localized Corrosion Susceptibility of Alloy 22 in Chloride Solutions

Ricardo M. Carranza, C. Mabel Giordano, Martín A. Rodríguez, Gabriel O Ilevbare¹ and Raul B. Rebak²

Comisión Nacional de Energía Atómica, 1650 San Martín, Buenos Aires, Argentina

¹Electric Power Research Institute, Palo Alto, CA, 94304, USA

²Lawrence Livermore National Laboratory, Livermore, CA, 94550, USA

ABSTRACT

Electrochemical studies such as cyclic potentiodynamic polarization (CPP) and electrochemical impedance spectroscopy (EIS) were performed to determine the corrosion behavior of Alloy 22 (N06022) in 1M NaCl solutions at various pH values from acidic to neutral at 90°C. All the tested material was wrought Mill Annealed (MA). Tests were also performed in NaCl solutions containing weak organic acids such as oxalic, acetic, citric and picric. Results show that the corrosion rate of Alloy 22 was significantly higher in solutions containing oxalic acid than in solutions of pure NaCl at the same pH. Citric and picric acids showed a slightly higher corrosion rate, and acetic acid maintained the corrosion rate of pure chloride solutions at the same pH. Organic acids revealed to be weak inhibitors for crevice corrosion. Higher concentration ratios, compared to nitrate ions, were needed to completely inhibit crevice corrosion in chloride solutions. Results are discussed considering acid dissociation constants, buffer capacity and complex formation constants of the different weak acids.

INTRODUCTION

Alloy 22 (N06022) contains by weight approximately 22% chromium (Cr), 13% molybdenum (Mo), 3% tungsten (W) and approximately 3% iron (Fe). Alloy 22 was commercially designed to resist the most aggressive industrial applications, offering a low general corrosion rate both under oxidizing and reducing conditions[1]. Under oxidizing and acidic conditions Cr exerts its beneficial effect in the alloy. Under reducing conditions the most beneficial alloying elements are Mo and W, which offer a low current for hydrogen discharge [2]. Due to its balanced content in Cr, Mo and W, Alloy 22 is used in hot chloride environments where austenitic stainless steels may fail by pitting corrosion and stress corrosion cracking (SCC) [1,2].

Alloy 22 is the material selected for the fabrication of the outer shell of the nuclear waste containers for the Yucca Mountain site [3,4]. Several papers have been published recently describing the general and localized corrosion behavior of Alloy 22 regarding its application for the nuclear waste containers [5]. It is also known that the addition of nitrate and other oxyanions to a chloride-containing environment, decreases or eliminates the susceptibility of Alloy 22 to localized attack [6,7]. It has been recently reported that fluoride ions may also act as an inhibitor to crevice corrosion of Alloy 22 [8]. Little is known on its corrosion behavior in organic acids [9].

Oxalic acid ($H_2O_4C_2$) is one of the most aggressive alkane acids and is slightly oxidizing. Acetic acid ($H_4O_2C_2$) is a weak monocarboxylic acid and is classified as a weak acid, because it does not completely dissociate into its component ions when dissolved in aqueous solutions. At a concentration of 0.1 M, only about 1% of the molecules are ionized. Citric acid ($C_6H_8O_7$) is a

weak tricarboxylic acid that shares the properties of other carboxylic acids. When heated above 175 °C, it decomposes through the loss of carbon dioxide and water. Citric acid is used in the biotechnology industry to passivate high purity process piping. Picric acid ($C_6H_3O_7N_3$) is an aromatic nitro compound ($ArNO_2$) which can be reduced to nitroso compounds ($ArNO$) or to hydroylamines ($ArNH_2$) by means of different reaction mechanisms [10]. The principal laboratory use of picric acid is in microscopy, where it is used as a reagent for staining samples.

Table I shows the dissociation K_a and metal complex formation K_{cpx} constants for the organic acids. It can be seen that oxalic acid is the strongest acid followed by picric, citric and acetic in decreasing acidity. For the same concentration oxalic acid will produce the lowest pH and acetic acid the highest one. The complexing character is more difficult to evaluate for it depends on the metal cation being complexed, the ionic strength of the solution and the temperature.

The objective of the current study was to use electrochemical methods and parameters to systematically assess the corrosion behavior of Alloy 22 (N06022) in sodium chloride solutions with additions of different organic acids as compared to the behavior in pure sodium chloride solutions of the same pH. General corrosion behavior was assessed by corrosion rate measurements using the Electrochemical Impedance Spectroscopy EIS technique, and localized corrosion behavior was evaluated using Cyclic Potentiodynamic Polarization CPP curves.

EXPERIMENTAL

Specimens of Alloy 22 were prepared from wrought mill annealed plate (MA) stock. The chemical composition of the alloy in weight percent was 59.20% Ni, 20.62% Cr, 13.91% Mo, 2.68% W, 2.80% Fe, 0.01% Co, 0.14% Mn, 0.002% C, and 0.0001% S. Two types of specimens were used: (a) prismatic specimens: a variation of the ASTM G 5 [11] specimen, and (b) prism crevice assemblies (PCA), fabricated based on ASTM G 48[11] which contained 24 artificially creviced spots formed by a ceramic washer (crevice former) wrapped with a PTFE tape. The applied torque was 7.92 N-m (70 in-lb). The PCA specimen has been described before [12]. The tested surface areas were approximately 10 cm² for prismatic specimens and 14 cm² for PCA specimens. The specimens had a finished grinding of abrasive paper N° 600, and were degreased in acetone and washed in distilled water. Polishing was performed 1 hour prior to testing. Electrochemical measurements were conducted in a three-electrode, borosilicate glass cell (ASTM G 5) [11]. A water-cooled condenser combined with a water trap was used to avoid evaporation and the ingress of air. Solution temperature was controlled by immersing the cell in a thermostated water bath. The cell was equipped with both a water cooled Luggin capillary and a saturated calomel reference electrode (SCE) which has a potential of 0.242 V more positive than the standard hydrogen electrode (SHE). A large area platinum wire was used as counter electrode. The electrochemical tests were carried out in 1M, 0.1M and 0.01M NaCl solutions, at different pH values between 1 and 6, with and without the addition of organic acids with concentrations from 0.001M to 2M. Small amounts of HCl were added in order to adjust solution pH of pure NaCl solutions. The test temperature was 90.0 ± 0.1°C. Solutions were prepared with analytical grade chemicals and 18.2 MΩ resistivity water. Solutions for the cyclic potentiodynamic polarization curves were deaerated with nitrogen. Solutions for EIS measurements were naturally aerated, that is, neither air nor nitrogen were purged through the solution.

Cyclic potentiodynamic polarization (CPP) curves (ASTM G 61) [11] were performed using PCA specimens. The potential scan was started at the end potential of a 10 minutes gal-

vanostatic cathodic treatment of $50 \mu\text{A}\cdot\text{cm}^{-2}$ in the anodic direction at a scan rate of 0.167 mV/s . The scan direction was reversed when the current density reached 5 mA/cm^2 in the forward scan. Solutions tested were NaCl solutions (0.01M to 1M) with and without the addition of organic acids (0.001 to 2M). The solutions were deaerated.

Table I. Dissociation [13] and metal complex formation [14,15] constants for organic acids. $M + nL \leftrightarrow ML_n$, M: metal ion, L: organic ligand, ML_n : metal complex. Parentheses: T °C (25°C when not indicated) and ionic strength of the solutions.

DISSOCIATION CONSTANTS		Acetic Acid Ethanoic $\text{CH}_3\text{CO}_2\text{H}$	Oxalic Acid $\text{C}_2\text{H}_2\text{O}_4$	Citric Acid $\text{C}_6\text{H}_8\text{O}_7$	Picric Acid $\text{C}_6\text{H}_3\text{O}_7\text{N}_3$
H^+	$\log K_{a1}$	-4.757	-4.266	-6.396	-0.33
	$\log K_{a2}$		-1.252	-4.761	
	$\log K_{a3}$			-3.128	
METAL COMPLEX FORMATION CONSTANTS K_{cpx}					
Cr^{2+}	$\log(\text{ML}/\text{M}\cdot\text{L})$	1.25 (0.3)	3.85 (0.1)		1.05 (18-25°C)
		1.80 (0)			
	$\log(\text{ML}_2/\text{M}\cdot\text{L}^2)$	2.15 (0.3)	6.81 (0.1)		
		2.92 (0)			
Cr^{3+}	$\log(\text{ML}/\text{M}\cdot\text{L})$	4.63 (0.3)			
	$\log(\text{ML}_2/\text{M}\cdot\text{L}^2)$	7.08 (0.3)			
	$\log(\text{ML}_3/\text{M}\cdot\text{L}^3)$	9.6 (0.3)			3.2 (18-25°C)
Co^{2+}	$\log(\text{ML}/\text{M}\cdot\text{L})$	1.10 (0.16)	3.84 (0.1)	5.00 (20°, 0.1)	
		0.71 (30°, 0.4)	3.25 (1.0)	4.83 (0.16)	
		0.81 (1.0)	4.72 (0)		
		1.40 (0)			
	$\log(\text{ML}_2/\text{M}\cdot\text{L}^2)$		5.60 (1.0)		2.85 (18-25°C)
			7.0 (0)		
	$\log(\text{MHL}/\text{M}\cdot\text{HL})$		1.61 (0.1)	3.02 (20°, 0.1)	
				3.19 (0.16)	
	$\log(\text{M}(\text{HL})_2/\text{M}\cdot(\text{HL})^2)$		2.89 (0.1)		
	$\log(\text{M}_2\text{HL}/\text{M}\cdot\text{H}_2\text{L})$			1.25 (20°, 0.1)	
Ni^{2+}	$\log(\text{ML}/\text{M}\cdot\text{L})$	0.74 (0.5)	5.16 (0)	5.40 (20°, 0.1)	2.89 (18-25°C)
		0.83-0.1 (1.0)		5.11 (0.16)	
		1.43 (0)			
	$\log(\text{MHL}/\text{M}\cdot\text{HL})$			3.30 (20°, 0.1)	
			3.19 (0.16)		
	$\log(\text{M}_2\text{HL}/\text{M}\cdot\text{H}_2\text{L})$			1.75 (20°, 0.1)	
Fe^{2+}	$\log(\text{ML}/\text{M}\cdot\text{L})$	1.40 (0)	3.05 (1.0)	4.4 (20°, 0.1)	
	$\log(\text{ML}_2/\text{M}\cdot\text{L}^2)$		5.15 (1.0)		
	$\log(\text{MHL}/\text{M}\cdot\text{HL})$			2.65 (20°, 0.1)	
Fe^{3+}	$\log(\text{ML}/\text{M}\cdot\text{L})$	3.38 (20°, 0.1)	7.53 (0.5)	11.50 (20°, 0.1)	1.8 (18-25°C)
		3.2 (20°, 1.0)	0.1 (0.1)		
		3.23 (3.0)	7.59 (1.0)		
			7.54 (3.0)		
	$\log(\text{ML}_2/\text{M}\cdot\text{L}^2)$	6.5 (20°, 0.1)	13.64 (0.5)		
		6.22 (3.0)			
	$\log(\text{ML}_3/\text{M}\cdot\text{L}^3)$	8.3 (20°, 0.1)	18.49 (0.5)		3.1 (18-25°C)
	$\log(\text{MHL}/\text{M}\cdot\text{HL})$		4.35 (0.5)		
	$\log(\text{M}_3(\text{OH})_2\text{L}_6/\text{M}^3\cdot(\text{OH})^2\cdot\text{L}^6)$				
	$\log((\text{ML})^2/\text{M}_2(\text{H}_1\text{L})_2\cdot\text{H}^2)$			1.6 (20°, 0.1)	

Electrochemical Impedance Spectroscopy (EIS) measurements were carried out at the corrosion potential in natural aerated solutions after 24h of immersion. The low frequency EIS polarization resistance (R_p) was used to calculate corrosion rates (CR) [8].

RESULTS

Figure 1 shows the general CR of Alloy 22 for pure 1M NaCl solutions from pH 1 to 6 and for 1M NaCl solutions with the addition of different concentrations of organic acids from 0.001M to 0.1M. The pH of the solutions containing organic acids was not modified and was the result of the normal organic acid identity and concentration. For pure chloride solutions, CR was very low and independent of solution pH for pH values between 2 and 6 ($CR \sim 0.1 \mu\text{m}\cdot\text{yr}^{-1}$). An increase of one order of magnitude was observed in the CR for pH 1 pure chloride solution ($CR \sim 1 \mu\text{m}\cdot\text{yr}^{-1}$). Compared to pure chloride solutions of similar pH: (a) CR was not modified by the addition of acetic acid for all the concentrations employed (0.1M, 0.01M and 0.001M), (b) CR was slightly increased by the addition of the higher concentrations of citric acid (0.1 and 0.01M) and picric acid (0.05M* and 0.01M), and (c) CR was significantly increased by the addition of oxalic acid for all the concentrations tested (0.1M, 0.01M and 0.001M) reaching the value of $24 \mu\text{m}\cdot\text{yr}^{-1}$ for the highest concentration.

Figure 2 shows CPP curves obtained using PCA specimens with crevice formers. All the curves presented a passive zone with low current densities from 1 to $10 \mu\text{A}\cdot\text{cm}^{-2}$. After the passive domain the increase of current densities with potential was due to crevice corrosion initiation and/or to transpassive dissolution. Current hysteresis was always observed between the forward and the reverse scans. The repassivation potential chosen was the cross-over potential E_{CO} , i. e. the potential at which the reverse scan intersects the forward scan.

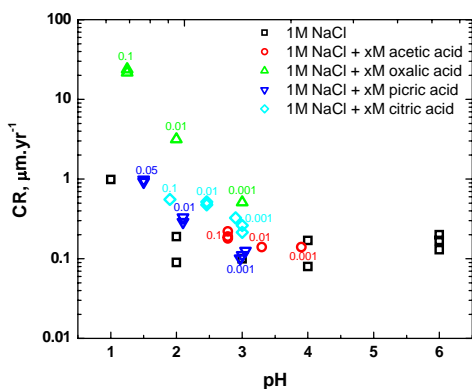


Figure 1. Corrosion rate, obtained from R_p EIS low frequency fitting parameter after 24h of immersion in naturally aerated solutions, as a function of pH and concentration of the added organic acid to 1M NaCl (figures next to symbols)

Abnormally high E_{CORR} values were obtained during the CPP curves in picric acid containing solutions (Figure 2). Consequently, the reverse scan intersected the forward scan in its cathodic domain. An extra cathodic reaction would produce misleading high E_{CO} values. Cyclic voltammetry (not shown) obtained at room temperature using a Pt electrode in deaerated 1M NaCl and 1M NaCl + 0.01M picric acid solutions both at pH 2, clearly demonstrate that the presence of picric acid significantly increased the cathodic current at potentials more anodic than the potential for hydrogen evolution reaction at the corresponding pH. This current increase was attributed to the picric acid reduction reaction [10]. Picric acid was then discarded for E_{CO} measurements. Crevice corrosion was observed in all the specimens in these solutions at the end of the CPP curves and the morphology of the attack can be observed in Figure 3. Typical shiny crystal-line attack was observed under the crevice formers generally under all the 24 teeth of the crevice formers. The grain structure of the alloy was also lightly revealed under the crevice formers.

* Higher concentrations of picric acid are not possible in aqueous solution due to solubility limitations.

Figure 4 shows the values of E_{CO} as a function of solution pH and organic acid concentration for deaerated 1M NaCl with and without addition of organic acids. A large dispersion of the results was obtained. E_{CO} values between 0 mV_{SCE} and -200 mV_{SCE} were obtained independently of solution pH, composition and organic acid concentration. Neither inhibiting nor detrimental effect on localized corrosion could be attributed to organic acids in the Set A solutions.

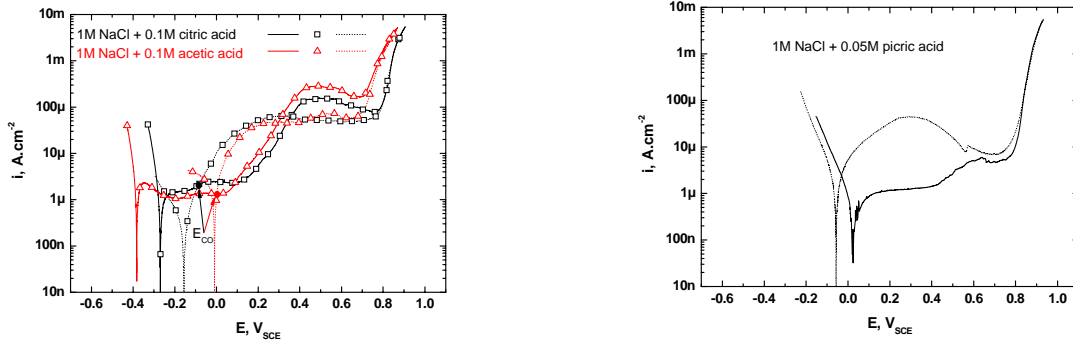


Figure 2. CPP curves for Alloy 22 at 90°C. Solid lines: forward scan. Dotted lines: reverse scan. E_{CO} : Cross-over repassivation potential.

Another set of CPP curves was run using higher ratios of organic acid concentration to chloride ion concentration $r_{org} = [Org]/[Cl^-]$ (Set B solutions). Set A solutions shown in Figure 4 correspond to r_{org} 0.1 to 0.001 (r_{org} is zero for pure chloride solutions). In Set B, r_{org} was increased to 1, 2, 5, 10 and 20. Solutions of Set B were equimolar organic acid + sodium organic salt (weak acid + conjugate base) solutions in order to have the highest possible buffer capacity in the solutions at those concentrations ($pH = pK_a$). $[Cl^-]$ was decreased to 0.1 and 0.01M when needed due to precipitation. Figure 5 shows a CPP curve obtained for high r_{org} Set B solutions. It can be seen that current hysteresis has disappeared in the tested specimens. No crevice attack was observed. Figure 6 shows E_{CO} as a function of r_{org} for all the solutions tested in the present work, including those already shown in Figure 4 (Sets A and B). The average E_{CO} for pure chloride solutions was also included in Figure 4 as horizontal dotted lines. A complete inhibition of crevice corrosion was obtained for: a) acetic+acetate solutions with r_{org} higher than 10, b) citric+citrate solutions with r_{org} higher than 2, and c) oxalic+oxalate solutions with r_{org} higher than 2. Transpassivity potentials E_{20} were also included in Figure 6. E_{20} corresponds to the potential at which the anodic current density reached the value of 20 $\mu A.cm^2$ in the forward scan of the CPP curves (Figure 5) when no crevice corrosion was found.

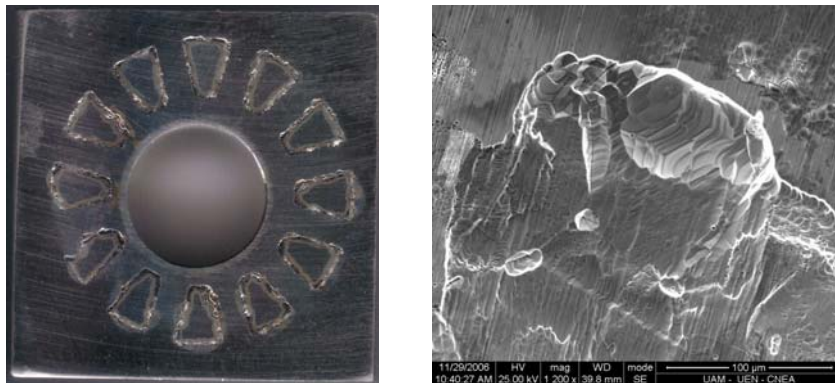


Figure 3. Optical and SEM images of Alloy 22 PCA specimen after CPP in deaerated 1M NaCl + 0.01M oxalic acid solution at 90°C.

DISCUSSION

As it is shown in Figure 1 only the addition of oxalic acid to chloride containing solutions significantly increased general CR of Alloy 22 if compared to pure chloride solutions at the same pH. This fact implies that an additional effect on the CR, besides the low pH value, is produced by the presence of oxalic acid. From the K_{cpx} found in the bibliography (Table I) it can be seen that the highest values of K_{cpx} correspond to oxalic and citric acids. However, no K_{cpx} were found for complexes formed with Cr cations and citric acid while for picric and oxalic acids values were found only for Cr^{+2} cations complexes. The complexing power of citric and oxalic acids with Ni cations is similar, and it diminishes following: oxalic \sim citric $>$ picric $>$ acetic. No K_{cpx} values were found for these organic acids and Mo cations. If it is assumed that passive films on Alloy 22 are enriched in Cr and Mo [16], the hypothesis that a higher general CR is due to a higher complexing character of the solution components for Mo, Cr and Ni, can not be simply ruled out. Instead, additional quantitative information about K_{cpx} together with identification of the cations forming the passive film at the open circuit potential must be obtained.

Results obtained using the CPP method showed that large concentrations of organic acids were necessary in order to obtain a complete inhibition of crevice corrosion in Alloy 22. Citrate and oxalate ions eliminated crevice corrosion for concentration ratios r_{org} higher than 2 while acetates needed r_{org} equal or higher than 10. Much lower inhibitor to chloride ratios r were published for nitrate, carbonate, bicarbonate, and sulfate anions ($r = [\text{Anion}]/[\text{Cl}^-] \approx 0.1$) to completely inhibit chloride induced crevice corrosion [17,18,19]. On the other hand, r higher than 2 are necessary to eliminate chloride induced crevice corrosion in fluoride containing solutions with a chloride concentration of 0.01M while r higher than 5 are needed for chloride concentrations of 0.1M and 1M.[12] If the localized acidification model is valid for crevice corrosion as was argued elsewhere [20], one would expect that the weaker the organic acid, the stronger is the inhibition if only chemical reactions are involved in the elimination of free protons. One would expect for example that acetate ions ($\log K_a = -4.757$) would be a better inhibitor compared to fluoride ions ($\log K_a = -3.15$) in contradiction with which it was found in this work. It can then be argued that small anions as fluoride enter easily into the crevice and hence they are more able to inhibit crevice corrosion. On the other hand, comparing the organic acids between them, the expected inhibiting strength according to K_a would be: acetic $>$ citric $>$ oxalic, which is not what was found in this work. The solutions used in the present work with r_{org} higher than 0.1 were prepared using equal molar concentrations of the organic acid and its corresponding sodium salt (conjugate base), in order to have the higher possible buffer capacity β . The higher the value of β the more difficult is to reduce the pH in the crevice to reach the low pH values needed to propagate it. The buffer capacity is independent of K_a and it is a function only of the total concentration of anions. It is then expected that different organic acids at $\text{pH} = \text{p}K_a$ (equal concentrations of the acid and its conjugate base) and the same total concentration have the same β and therefore, the same crevice corrosion inhibiting effect. The observed differences could be attributed to differences in molecular size as it was previously invoked for fluoride ions. If we consider molecular sizes, the inhibiting power should vary following: acetic $>$ oxalic $>$ citric. Experimental results showed that larger citric and oxalic acids were better inhibitors than the smaller acetic acid, even though the total oxalate concentration was lower (lower β) than the total acetate concentration, under complete inhibition conditions (Figure 6).

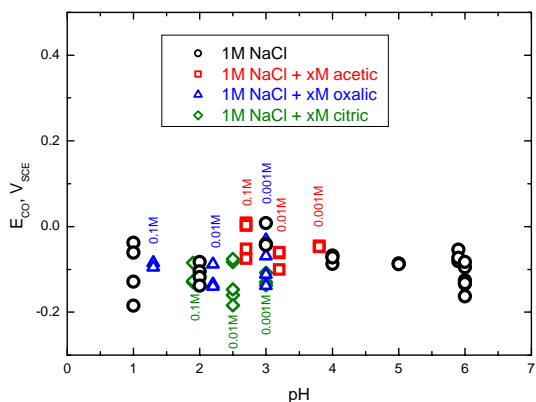


Figure 4. Cross-over Repassivation Potential as a function of solution pH. Deaerated solutions at 90 °C.

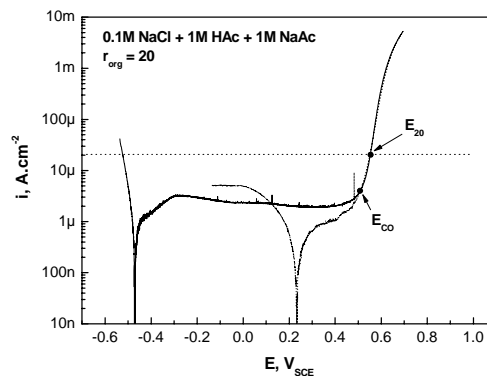


Figure 5. CPP curve for Alloy 22 at 90°C. Solid lines: forward scan. Dotted lines: reverse scan.

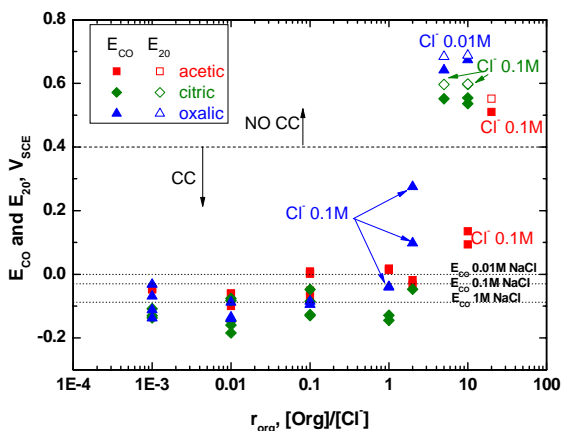


Figure 6. Cross-over repassivation potential and transpassive potential as a function of the ratio of organic inhibitor concentration to chloride ion concentration $r_{org} = [Org]/[Cl^-]$. Full symbols: E_{CO} . Empty symbols: E_{20} . Dotted lines: mean E_{CO} for pure chloride solutions. Dashed line: E_{CO} limit for crevice corrosion.

Consequently, differences in localized corrosion inhibition can not be easily attributed to differences in K_a , β or molecular sizes. A systematic study with other organic and inorganic compounds must be undertaken in order to elucidate the mechanism involved in crevice corrosion inhibition in Alloy 22. This systematic study must include a modeling of the concentration profile inside the crevice for all the species present in solution.

SUMMARY

The general corrosion rates of Alloy 22 after 24-h of immersion in 1M NaCl solutions with the addition of oxalic acid in concentrations ranging from 0.1M to 0.001M were higher than those obtained for pure 1M NaCl solutions at the same pH, while the addition of the same concentrations of acetic acid produced no changes in the corrosion rate. The addition of citric and picric acids produced a slight increase of the corrosion rate at the highest concentrations used. Additional tests are needed in order to determine with certainty whether or not an increase in general corrosion rate of Alloy 22 can be attributed to a high metal complexing strength of an organic ligand.

Large concentrations of organic anions were needed in order to eliminate crevice corrosion in Alloy 22 in chloride solutions. Crevice corrosion was completely inhibited for r_{org} values higher than 10 in acetate/chloride solutions and higher than 2 for oxalate/chloride and citrate/chloride

solutions. The differences in inhibition strength could not be clearly associated to the dissociation constants of the acids, nor to their buffer capacities or to their molecular sizes.

ACKNOWLEDGEMENTS

R. M. Carranza acknowledges financial support from the Agencia Nacional de Promoción Científica y Tecnológica of the Ministerio de Educación, Ciencia y Tecnología from Argentina. This work was performed under the auspices of the U. S. Department of Energy by the University of California Lawrence Livermore National Laboratory under contract N° W-7405-Eng-48. This work is supported by the Yucca Mountain Project, which is part of the Office of Civilian Radioactive Waste Management (OCRWM).

REFERENCES

1. R.B. Rebak and P. Crook, "Influence of the Environment on the General Corrosion Rate of Alloy 22 (N06022)", Proc. Pressure Vessels and Piping Conf., 25-29 July 2004, San Diego, CA, PVP-Vol. 483, p. 131 (ASME, 2004: New York, NY).
2. R.B. Rebak in Corrosion and Env. Degradation, Vol. II, p. 69 (Wiley-VCH, 2000, Germany).
3. G.M. Gordon, Corrosion, 58, 811 (2002).
4. Yucca Mountain Science and Engineering Report, U. S. Department of Energy, Office of Civilian Radioactive Waste Management, DOE/RW-0539, Las Vegas, NV, May 2001.
5. R.B. Rebak, Paper 05610, Corrosion/2005 (NACE International, 2005: Houston, TX).
6. D.S. Dunn, L. Yang, C. Wu, G.A. Cragnolino, Mat. Res. Soc. Symp. Proc. Vol 824 (MRS, 2004: Warrendale, PA)
7. D.S. Dunn, Y.-M. Pan, K. Chiang, L. Yang, G.A. Cragnolino and X. He, "Localized Corrosion Resistance and Mechanical Properties of Alloy 22 Waste Package Outer Containers" JOM, January 2005 (TMS, 2005: Warrendale, PA)
8. R.M Carranza, M.A. Rodríguez, R.B. Rebak, Paper 06622, Corrosion/2006 (NACE Int., 2005: Houston, TX).
9. S.D. Day, M.T. Whalen, K.J. King, G.A. Hust, L.L. Wong, J.C. Estill, R.B. Rebak, Corrosion, 60, 804 (2004).
10. J. March, Adv. Organic Chemistry, Reactions, Mechanisms, and Structure. 3rd Ed., J. Wiley & Sons, p. 1103, N.Y., 1985.
11. Annual Book ASTM Standards, vol. 03.02 (West Conshohocken, PA: ASTM Int. 2005).
12. R.M. Carranza, M.A. Rodríguez, R.B. Rebak, Corrosion, 63, 480 (2007).
13. CRC Handbook of Chem. and Phys., David R. Lide, Ed., 85th Ed., CRC Press, NY, 2004.
14. Critical Stability Constants, R.M. Smith and A.E. Martell, eds., Plenum Press, NY, 1976.
15. Stability Constants, Part I: Organic Ligands, J. Bjerrum, G. Schwarzenbach, and L.G. Sillén, eds., The Chemical Society, London, 1957
16. A.C. Lloyd, J.J. Noël, S. McIntyre, D.W. Shoesmith, Electrochim. Acta 49, 3015 (2004).
17. D.S. Dunn, O. Pensado, and G.A. Cragnolino, Paper 05588, Corrosion/2005 (NACE Int., 2005: Houston, TX).
18. D.S. Dunn, Y.-M. Pan, L. Yang and G.A. Cragnolino, Corrosion, 61, 1078 (2005).
19. D.S. Dunn, Y.-M. Pan, L. Yang and G.A. Cragnolino, Corrosion, 62, 3 (2006).
20. R.M Carranza, M.A. Rodríguez, R.B. Rebak, Paper 07581, Corrosion/2007 (NACE Int., 2007: Houston, TX).